Chemie der Erde 75 (2015) 301–315

Contents lists available at ScienceDirect

Chemie der Erde

journal homepage: www.elsevier.de/chemer

Sr and Nd isotopes as tracers in pedogenic studies: Evidence for Saharan dust contribution to the soils of Muravera (Sardinia, Italy)

Francesca Castorina[a,b,*], Umberto Masi[b]

[a] Dipartimento di Scienze della Terra, University of Rome "La Sapienza", Piazzale A. Moro 5, I-00185 Rome, Italy
[b] IGAG – Istituto di Geologia Ambientale e Geoingegneria – CNR c/o Dipartimento di Scienze della Terra, University of Rome "La Sapienza", Piazzale A. Moro 5, I-00185 Rome, Italy

ARTICLE INFO

Article history:
Received 14 December 2012
Accepted 25 April 2015
Editorial handling - S. Norra

Keywords:
Sr–Nd isotopes
Unpolluted soils
Metamorphic rocks
Pedogenesis
Sr–Nd sources
Saharan dust
Muravera
Sardinia

ABSTRACT

Sr and Nd isotopes were applied to 5 soil profiles from the Muravera area, in south-eastern Sardinia.

All the soils, which have developed during the Quaternary on the Lower Paleozoic metamorphic basement except for one on Eocene carbonates, are located far from major sources of pollution. Therefore, they are suitable for testing pedogenic processes and geochemical evolution to benefit for environmental studies.

The Sr isotopic ratios range largely ($\delta^{87}Sr = 1.7–65.9‰$), even in each soil profile. In particular, the observed increase of $\delta^{87}Sr$ with depth in the most of the metamorphic rock-based soils can be accounted for by the downward decrease of Sr contributions from organic matter and Saharan dust, both displaying lower isotopic ratios than the soil bedrocks. The carbonate rock-based soil exhibits $\delta^{87}Sr$ higher (1.7–18.1‰) than the bedrock, indicating a significant contribution of radiogenic Sr from the siliciclastic fraction of the soil, and probably from dust input. The Nd isotopic ratios are slightly variable through the profiles (ε_{Nd} from −7.8 to −14.5), confirming little mobility of Nd and Sm during the pedogenesis. Among the minerals present in the soils, phosphates, albite, and calcite are those important in providing low radiogenic Sr and Nd to organic matter of the soils.

Lastly, this isotopic study has in particular allowed for evaluating the potential proportion of contribution of Saharan dust to south-eastern Sardinia, thus corroborating the findings of other studies related to soils from the central-western Mediterranean.

1. Introduction

Unlike in other Countries (e.g. Borg and Banner, 1996; Steinmann and Stille, 1997; Martin and McCulloch, 1999; Kurtz et al., 2001; Aubert et al., 2002; Pett-Ridge et al., 2009; Stille et al., 2009), the coupled application of Sr and Nd isotopes to the study of soils is still a novelty in Italy (Castorina and Masi, 2007, 2008). In particular, Sr isotopes have been applied to soil sciences since the late 1980s (e.g. Åberg et al., 1989; Blum and Erel, 1997; Bullen et al., 1997; Capo et al., 1998; Stewart et al., 1998; Vitousek et al., 1999; Green et al., 2004; Poszwa et al., 2004; Drouet et al., 2005), showing that they can be important tracers applicable not only to large-scale ecosystem studies, but also to short-scale to describe chemical weathering, pedogenesis, cation provenance, and mobility. The application of Nd isotopes as tracers of rock weathering processes and mobilization of rare earth elements (REE) in soils is more recent, probably because REE have long been considered immobile in the most of supergenic processes. It has been emphasized that the Nd isotopic composition dominantly reflects the provenance of soil components (e.g. Borg and Banner, 1996; Steinmann and Stille, 1997; Öhlander et al., 2000; Viers and Wasserburg, 2004; Roig et al., 2006). In particular, Öhlander et al. (2000) showed that Nd is preferentially released from minerals with a lower Sm/Nd ratio than the bulk soil, leading to lower $^{143}Nd/^{144}Nd$ ratio in the initial stages of weathering. Viers and Wasserburg (2004) demonstrated that the soil evolution involves the differential dissolution of primary phases of the parent rock, surface waters, and the atmospheric REE input via dust from even far regions, as well as the formation of diagenetic phases, particularly phosphates, indicating contributions from different reservoirs to soils. Nevertheless, the mechanisms controlling the REE fractionation and mobility in soils are still not fairly understood.

* Corresponding author at: Dipartimento di Scienze della Terra, University of Rome—La Sapienza, Piazzale A. Moro 5, 00185 Roma, Italy. Tel.: +39 06 49914146; fax: +39 06 4454729.
E-mail address: francesca.castorina@uniroma1.it (F. Castorina).

http://dx.doi.org/10.1016/j.chemer.2015.04.003
0009-2819/

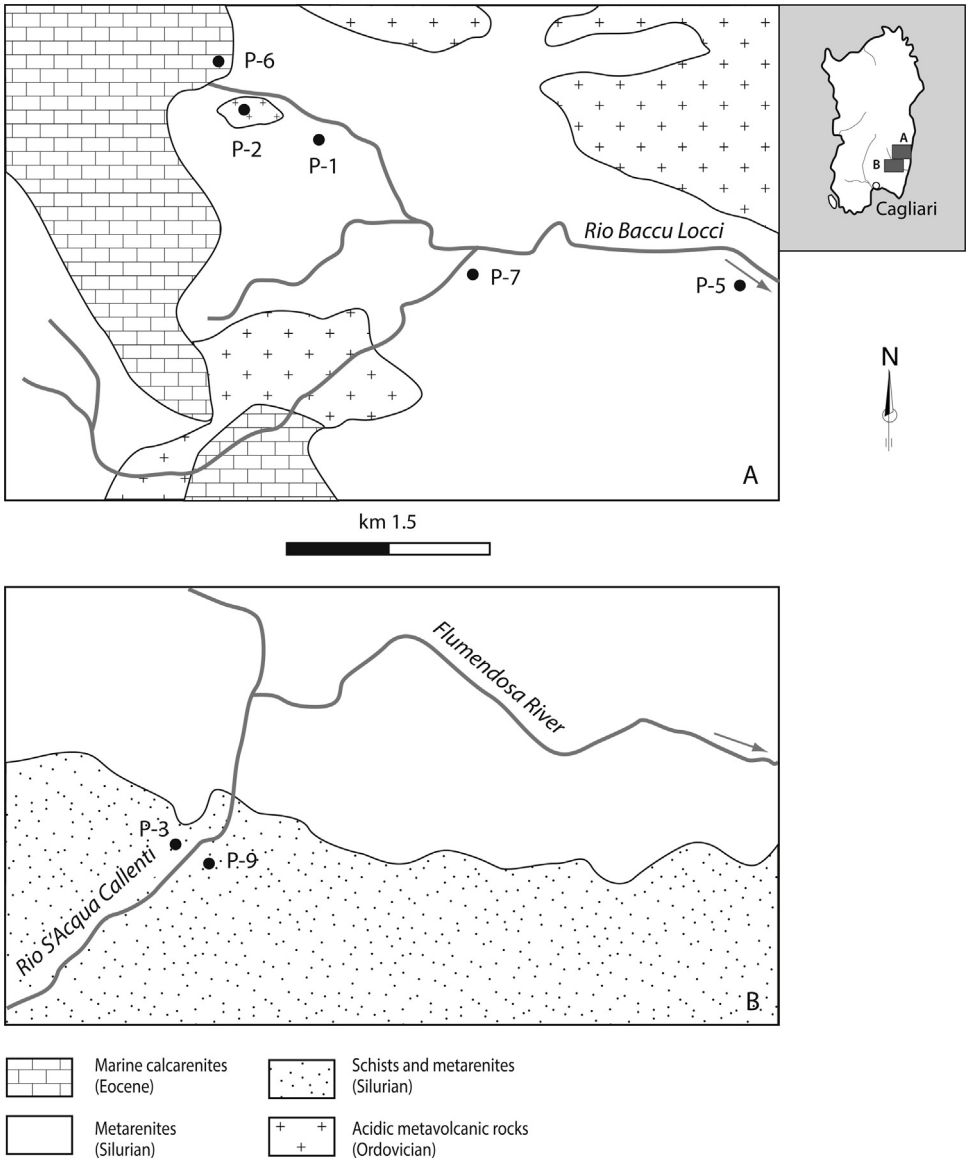

Fig. 1. Geological sketchy map of the study areas near Muravera (modified after Carmignani et al., 2001) showing the locations of the studied soils. The area depicted in (A) lay about 15 km NE of the area shown in (B). The locations of the P-3 and P-5 soils from the same territories (Castorina and Masi, 2007, 2008) are also shown (see text). The inset map shows the location of the study areas in Sardinia.

This paper presents a study conducted on 23 samples collected from 5 profiles located in the Muravera area, south-eastern Sardinia (Fig. 1), aimed at defining the bearing of Sr and Nd isotopes on the pedogenic and geochemical evolution of those soils. As the study area is remote from major sources of pollution such as industries, traffic, animal husbandry, agriculture, and towns, it provides a good test for studying natural processes. Moreover, as almost all the soils, although displaying different stages of pedogenesis, have developed on the same bedrock represented by the Lower Paleozoic metarenites known as *Arenarie di san Vito* (Scarciglia et al., 2013), this can be useful for tracing the soil evolution through time.

Another major goal of this paper is the estimation of the potential aeolian deposition of dust on the soils. In this context, a number of papers unveiled that deserts provide significant material to the most of soils throughout the world (e.g. Spencer et al., 1995; Kurtz et al., 2001; Aubert et al., 2002; Nakano et al., 2004; Lahd Geagea et al., 2008b; Lawrence et al., 2011), including the Mediterranean area (e.g. Moulin et al., 1997; Yaalon, 1997; Nicolás et al., 2008; Erel and Torrent, 2010). In particular, Nicolás et al. (2008) found that Saharan dust makes up to 5–40% of the total concentration of PM_{10} deposited on southern Spain, and Erel and Torrent (2010) were the first researchers to have applied Sr isotopes to recognize the significant (33–86% in Al–silicates of the fine soil fraction) contribution to two soils from such area. In the Mediterranean, Sardinia is a favorable land for ascertaining the potential aeolian deposition, laying on storm trajectories from the Sahara to central Europe. The first study on aeolian deposits (from unknown sources) on Sardinian soils was carried out by Sevink and Kummel (1984). Later, Le-Bolloch et al. (1996) estimated that the present-day dust deposition on southern Sardinia ranges between 6 and 13 g/m^2. The Saharan contribution, although of modest magnitude, was also documented in paleosoils from the island by Genova et al. (2001) and Andreucci et al. (2012).

Lastly, the Sr isotopic data of the studied soils have been merged with those of two other profiles from the same area, developed on the same bedrocks (Castorina and Masi, 2007, 2008), thus obtaining a more representative set of data to corroborate the conclusions of this paper. We have also compared the Sr–Nd isotopic characteristics of the Sardinian soils with those of soils from other areas,

developed on similar bedrocks, to recognize potential common patterns of evolution.

As a whole, this isotopic study provides a basic information for understanding not only the natural processes taking place in soils unaffected by pollution, but also evaluating the potential proportion of the aeolian contribution from the Sahara. The results obtained have allowed us to corroborate the findings of Erel and Torrent (2010), providing new data on the diffusion of Saharan dust through the central Mediterranean.

2. Soil sampling and the sources of Sr and Nd in the area

The studied soil samples were collected horizon-wise from 10 profiles, which are representative of the main different soil types associated with the major landscape units (Scarciglia et al., 2011), in collaboration with researchers of soil science, who provided the relative description (e.g. Scarciglia et al., 2011, 2013). However, only the samples from 5 out of 10 profiles were analyzed for Sr and Nd isotopic ratios in this paper, and the Sr isotopic data were compared with those of the samples from other 2 profiles (out of 10) analyzed with the same procedure here described by Castorina and Masi (2007, 2008). In addition to the soil samples, three samples of marine aerosol from three sites of the nearby Tyrrhenian coast along with a sample of seawater have been analyzed for Sr isotopic composition. No determination has been carried out for Nd isotopic composition, as seawater and marine aerosols contain negligible concentrations of REE (e.g. Tanaka and Kawabe, 2006).

The studied soils are located in south-eastern Sardinia, north of the Muravera village, in the maximum range from the seacoast of about 10 km for the soils of the catchment of the *Rio Baccu Locci* creek, and about 17 km for the P-9 soil from the valley of the *Rio S'Acqua Callenti* creek (Fig. 1). The area, which is characterized by elevations between 500 and 650 m a.s.l. (Scarciglia et al., 2011), is subjected to a semi-arid climate (mean annual rainfall about 700 mm mainly in autumn and springtime, and dry warm summers). All the soils, which are little or nil anthropized being far away from potential sources of pollution, are generally left to animal pasture, and are covered by the typical Mediterranean vegetation. The soils have developed on Quaternary deposits from the Lower Paleozoic metamorphic basement, except for the P-6 soil developed on Eocene calcarenites. In particular, the P-7 and P-9 soils occur on a slope deposit and a conoid, respectively, of the Pleistocene; both are characterized by well differentiated and strongly leached profiles with illuviation clay in the argillic (Bt) horizons. In contrast, where slope dynamics prevail as for the P-1 and P-2 soils developed on Holocene deposits, the profiles are of the A-Bw-R type (R is the little or nil weathered bedrock). The C horizon occurs only where morphology is steady as for the thick P-6 soil developed on a summit plateau. All the soils are, to variable extent, reddish, suggesting that they formed under more humid conditions compared with nowadays. Table 1 reports the main pedological and mineralogical characteristics of the soils after Scarciglia et al. (2013) along with the granulometric and chemical data obtained from this work. Detailed information, particularly concerning soil classification and exchangeable cations, is reported by Scarciglia et al. (2011).

The main sources of Sr and Nd in the study area are bedrock minerals, runoff, and atmospheric wet (marine aerosol) and dry (dust) depositions. Among them, bedrock minerals are by far quantitatively the most important source for the amount of Sr and Nd released by weathering to the soil solution. Runoff represents a potential source of Sr, but not of Nd, as REE are generally little soluble in water. However, the amount of Sr carried by runoff is comparatively very subordinate. Marine aerosol can provide little Sr and negligible Nd, as this latter along with the other REE are contained in seawater in very low concentrations (e.g. Tanaka and Kawabe, 2006). In contrast, dust from either local and far sources can provide a variable range of Sr and Nd amount from different rock-types. In particular, the local sources of dust are represented by the main rock formations of the area, i.e. sandstones, schists, and, subordinately, marine carbonates, whereas the far sources are represented by Saharan rocks and occasional ash from Sicilia's volcanoes. The details of the geochemical and isotopic characteristics of the main sources of Sr and Nd will be dealt in the Discussion.

3. Analytical procedure

After removing small pebbles, the soil samples were air-dried, sieved, and the fraction <2 mm was dried in an oven for 12 h at 105 °C to drop residual moisture. The determination of soil pH was carried out in water, whereas the granulometric analysis was obtained according to standard procedure based on Stokes Law. Organic C (C_{org} hereinafter) was determined by wet oxidation of the samples at 160 °C with 1/3 M $K_2Cr_2O_7$ (Springer and Klee, 1954), averaging 3 titration results. Sr, Ca, Fe_{tot}, Mn, and PO_4^{3-} were extracted from the fraction <2 mm of the samples after 2-step dissolution with an acid mixture. In step 1, about 0.5 g of each sample was digested in Teflon vials with 8 ml HF (50% v/v), 2 ml HNO_3 (67% v/v), and 2 ml $HClO_4$ (70% v/v) at 70 °C for 48 h, then evaporated to dryness, and converted into chloride using 6 N HCl. In step 2, the procedure was repeated at 200 °C to total digestion of the samples. All the used acids were of Suprapur™ grade, and were further purified by sub-boiling distillation. The solutions were prepared with Milli-Q grade water. Element concentrations, except for PO_4^{3-} measured colorimetrically, were determined using a Varian ICP-AES (Vista MXP Rad) at the Dipartimento di Scienze della Terra, University of Rome "La Sapienza". SRM-1643d and USGS QLO-1 standards were used to test accuracy and precision of the measurements, which were better than ±5%. The estimated detection limits were quantified via duplicates and blanks after each run of 10 samples. Nd concentrations were measured via ID using a ^{150}Nd spike solution. Sr and REE for isotopic analyses were separated in a 3 ml AG 50 W-X8 resin column. Nd was separated from the other REE in 2-ml columns filled with hydrogen di-ethylhexylphosphate (HDEHP)-coated Teflon powder (White and Patchett, 1984).

The aerosol samples were collected on Whatman 41© cellulose filters according to Arimoto et al. (1992)'s procedure, and were then dissolved with 2.5 ultrapure HC1 at room temperature. The seawater sample along with the aerosol solutions were centrifuged, and Sr, after separation from the matrix using standard procedure, was analyzed for isotopic composition by mass spectrometry.

Isotopic analyses were carried out at IGAG-CNR c/o Dipartimento di Scienze della Terra, University of Rome "La Sapienza" using a FINNIGAN MAT 262RPQ TIMS system (Thermal Ionisation Mass Spectrometry) of Thermo Scientific multicollector mass spectrometer with Re double filaments in static mode. Internal precision (within-run precision) of the single analytical value is given as two standard error of the mean. Repeated analyses of standards gave averages and errors expressed as two standard deviation (2σ) as follows: NBS 987 $^{87}Sr/^{86}Sr = 0.710241 \pm 0.000013$ ($n = 20$), $^{86}Sr/^{88}Sr$ normalized to 0.1194; La Jolla $^{143}Nd/^{144}Nd = 0.511860 \pm 0.000010$ ($n = 20$), and $^{146}Nd/^{144}Nd$ normalized to 0.7219. Correction for decay of ^{87}Rb and ^{147}Sm is unnecessary because of the young age of the soils. Total procedural blanks were below 2 ng Sr and 1 ng Nd for all the samples. Sr isotopic ratios, which are expressed as δ ‰ values relative to modern seawater standard, were calculated according to the following formula:

$$\delta^{87}Sr = \left[\left(\frac{^{87}Sr/^{86}Sr_{sample}}{^{87}Sr/^{86}Sr_{seawater}} \right) - 1 \right] \times 1000 \quad (1)$$

Table 1
The mineralogical and granulometric compositions, a selection of chemical data, and the soil classification (US Soil Taxonomy, quoted from Scarciglia et al., 2011) of the studied soil samples from Muravera. The available data of the P-3 and P-5 soils (Castorina and Masi, 2007, 2008) and their soil classification (Scarciglia et al., 2011) have been reported for comparison. The Nd contents of the P-3 soil samples have been determined in this work, whereas the Nd contents of the P-5 soil samples (in italics) refer to the clay soil fraction only (Scarciglia et al., 2011). Detection limits for Sr, Nd, Ca, $Fe_{tot.}$, Mn, and P were 0.2 mg/kg, 0.1 mg/kg, 0.1 mg/kg, 30 mg/kg, 5 mg/kg, and 0.1 mg/kg, respectively.

Soil and location	Horizon	Depth (cm)	Soil classification	Bedrock	Mineralogical composition	Notes	%			pH	(mg/kg)		(g/kg)	(wt%)			
							Sand	Silt	Clay		Sr	Nd	C_{org}	Ca	Fe_{tot}	Mn	P_2O_5
P-1 *Baccu Locci*	A1	0–4	Lithic Ultic		Qtz (>60%), Ms	Calcareous	43.1	47.9	9.0	5.8	114	25	90.5	1.37	4.35	0.137	0.26
	A2	4–20	Haploxeroll		(++) Ab (+), Kfs	debris and	40.8	43.2	16.0	6.3	111	24	65.0	0.50	4.69	0.174	0.15
	Bw	20–40			(+), accessory	Pb-As sulfides	53.9	29.1	17.0	6.3	93	31	25.0	0.06	5.28	0.035	0.10
	R	>40		*Arenarie di san Vito (metarenites)*	phases: Chl, Ap, Mnz, Xtm, Ill, Kln, Fe-Mn oxi-hydroxides						70	32		0.01	3.60	0.006	0.08
P-2 *Baccu Locci*	A1	0–3	Lithic Dystroxerept		As in the P-1 soil but more Kfs	As in the P-1-soil	52.4	34.6	13.0	6.0	71	15	57.8	0.39	2.65	0.114	0.18
	A2	3–15					44.4	38.6	17.0	6.1	74	18	34.0	0.30	3.00	0.119	0.19
	Bw	15–30					49.5	33.5	17.0	5.7	60	19	19.0	0.10	3.04	0.043	0.15
	R	>30		*Porphyroids (metarhyolites)*							30	6		0.01	0.47	0.001	0.03
P-6 *Baccu Locci*	A	0–7	Typic Haploxerept		Cc (> 80%) silicates and oxides	Fresh vegetal remains	33.2	54.0	12.8	7.4	88	38	78.0	1.60	3.92	0.047	0.10
	Bw1	7–45					21.4	57.0	21.6	7.4	241	17	14.5	0.40	4.60	0.044	0.03
	Bw2	45–62					36.0	35.3	28.7	7.7	238	31	7.2	13.00	4.27	0.023	0.03
	C1	62–80					40.4	37.7	21.9	8.1	92	27	6.8	17.24	3.15	0.013	0.04
	Cg2	80–102					15.0	47.1	37.9	8.0	387	31	8.1	7.25	2.93	0.014	0.04
	R	>102		*Calcarenites of Mt. Cardiga*							381	20		24.50	2.20	0.009	0.01
P-7 *Baccu Locci*	Oi	+2–0	Ultic		As in the P-1 soil												
	A	0–15	Haploxeralf			Fresh vegetal remains	35.9	47.1	17.0	6.3	70	20	49.1	0.39	1.35	0.027	0.10
	Bt1	15–40				Pedogenic clay	30.2	45.8	24.0	6.1	39	24	9.5	0.11	1.65	0.017	0.03
	Btg2	40–140				Pedogenic clay	37.8	39.2	23.0	5.8	55	19	2.0	0.02	2.09	0.015	0.01
	Btg3	140–200				Pedogenic clay	53.6	34.4	12.0	6.2	50	24	1.2	0.01	1.73	0.015	0.01
	Btg4	>200		Slope deposit on *Arenarie di san Vito*		Pedogenic clay	54.6	25.4	20.0	6.5	49	20	1.2	0.01	2.15	0.014	0.03
P-9 *S'Acqua Callenti*	A1	0–2	Haplic		As in the P-1 soil		56.6	30.4	13.0	5.9	57	17	51.4	0.19	3.90	0.045	0.25
	A2	2–14	Palexeralf				54.2	26.8	19.0	6.0	40	14	12.6	0.05	4.14	0.048	0.11
	Btg1	14–105				Pedogenic clay	54.7	12.3	33.0	5.7	60	22	1.1	0.03	6.35	0.033	0.08
	Btg2	105–155		Conoid on *Arenarie di san Vito*		Pedogenic clay	55.1	15.9	29.0	5.6	25	19	0.5	0.01	5.60	0.052	0.10
P-3 *S'Acqua Callenti*	Oi	2–0	Lithic		Qtz (+++), Ms						162	nd		0.58			
	A	0–20	Haploxeroll		(++) Ab (+), Cpx		45.8	38.3	15.9	6.2	143	14		0.30			
	Bw	20–26					52.1	35.6	12.3	6.5	157	21		0.19			
	R	>26		Slope deposit on *Arenarie di san Vito*							143	14		0.03			
P-5 *Baccu Locci*	Oi	4-0	Typic		Qtz (+++), Ms						90	nd		0.12			
	A	0–12	Herofluvent		(++) Chl (+), Ab		90.1	5.7	4.2	6.8	83	*35.0*		0.05			
	2Ab	12–19			(+), Kfs		55.6	34.9	9.5	6.2	85	*35.6*		0.10			
	2Bwb	19–25					80.4	15.9	3.7	6.0	72	*18.7*		0.04			
	3Cb	25–38					94.3	3.6	2.1	6.1	77	*33.6*		0.02			
	4Ab1	38–43					71.0	20.1	8.9	6.7	80	*30.2*		0.05			
	4Ab2	43–50					61.0	30.2	8.8	6.7	76	*34.6*		0.07			
	5Cb	50–100		Fluvial deposit			87.5	8.7	3.8	7.2	80	*38.2*		0.03			

quartz (Qtz), muscovite (Ms), albite (Ab), K-feldspar (Kfs), clinopyroxene (Cpx), calcite (Cc), chlorite (Chl), apatite (Ap), monazite (Mnz), xenotime (Xtm), illite (Ill), kaolinite (Kln).

where $^{87}Sr/^{86}Sr_{seawater} = 0.70917$ (Ricther and DePaolo, 1987). The measured $^{143}Nd/^{144}Nd$ ratios are presented as fractional deviation in parts in 10^4 (ε-units) from $^{143}Nd/^{144}Nd$ in a Chondritic Uniform Reservoir (CHUR) as measured today:

$$\varepsilon_{Nd(0)} = \left[\left(\frac{\left(^{143}Nd/^{144}Nd\right)_{sample}}{\left(^{143}Nd/^{144}Nd\right)_{CHUR}} \right) - 1 \right] \times 10^4 \quad (2)$$

where $(^{143}Nd/^{144}Nd)_{sample}$ is the ratio measured in the sample today and $(^{143}Nd/^{144}Nd)_{CHUR}$ is the ratio in the CHUR reference reservoir today, i.e. 0.511847 (DePaolo and Wasserburg, 1976).

4. Results

The data of granulometric analysis, pH, and the contents of Sr, Nd, C_{org}, Ca, Fe_{tot}, Mn, and P_2O_5 in the studied soils are reported in Table 1, whereas the Sr and Nd isotopic ratios are shown in Table 2, which also includes the Sr isotopic data of the marine aerosols and Tyrrhenian seawater. Table 1 also reports the soil classification after US Soil Taxonomy (quoted by Scarciglia et al., 2011). The element contents and the Sr–Nd isotopic ratios are graphically presented versus depth for each soil profile in Figs. 2 and 3, respectively.

The clay fraction is generally less abundant in all the soils relative to the sum of sand and silt. However, the clay fraction displays higher proportions in the more evolved soils. The sand fraction is more abundant than the silt fraction in the P-2 and P-9 soils, and in the lower horizons of the P-1 and P-7 soils.

All the metamorphic rock-based soils display sub-acidic reaction with overall pH values ranging narrowly from 5.6 to 6.5, whereas the carbonate-based P-6 soil exhibits neutral to sub-alkaline reaction with depth.

The Sr range is wide from 25 to 387 mg/kg in the metamorphic rock-based soils, where it generally exhibits a decrease with depth. In the carbonate-based P-6 soil, Sr increases toward the lower horizons, except for the C1 horizon characterized by a significant depletion. The range of Nd is narrow from 14 to 38 mg/kg; in particular, the more developed P-9 soil shows the narrowest range, whereas the carbonate-based P-6 soil displays the largest one. The Nd concentrations are generally high in the B horizons, except for the P-6 soil exhibiting enrichment in the A horizon. The C_{org} contents range overall widely from 0.5 to 90 g/kg, decreasing systematically with depth as usually observed in soils; in particular, the more developed P-7 and P-9 soils display the lowermost values in the B horizons. The Ca concentrations range widely from 0.01 to 17.24 wt%, and decrease systematically with depth in the metamorphic rock-based soils. In the carbonate-based P-6 soil, Ca is particularly low in the two uppermost horizons. The Fe_{tot} contents, which are higher in the B horizons as usually observed in soils, range between 1.35 and 6.35 wt%, displaying higher values in the P-1 and P-9 soils, and lower in the P-7 soil. The P-9 soil displays the largest range (3.9–6.35 wt%). Lastly, Mn (0.03–0.17 wt%) and P_2O_5 (0.01–0.26 wt%) are concentrated in the A horizons, exhibiting higher values in the less developed P-1 and P-2 soils, and, conversely, lower in the more evolved P-7 soil. The P-1 soil displays the widest Mn range (0.04–0.17 wt%). The P_2O_5 ranges are narrow in almost all the soils, among which the P-1, P-2, and P-9 soils display higher values than the other two soils of similar contents. The Mn and P_2O_5 contents generally decrease with depth in all the soils.

As shown by Fig. 4, the metamorphic rock-based soils display significantly positive correlations of Sr versus C_{org}, Ca, and Mn ($r^2 = 0.73$, 0.67, and 0.66, respectively) in the A horizons, whereas there is only the positive correlation with C_{org} ($r^2 = 0.51$) in the B horizons. Regarding Nd, the metamorphic rock-based soils exhibit a highly positive ($r^2 = 0.94$) correlation with C_{org}, and subordinate positive correlations with Ca and Mn ($r^2 = 0.62$ and 0.33, respectively) in the A horizons, whereas there is only the positive low correlation with C_{org} ($r^2 = 0.35$) in the B horizons (Fig. 4). A very good Sr–Nd positive correlation is apparent in the A horizons ($r^2 = 0.86$), and one subordinate ($r^2 = 0.45$) in the B horizons. Lastly, from Fig. 4, it appears that Ca displays a good positive correlation with C_{org} ($r^2 = 0.75$), and significantly lower correlations with P_2O_5 ($r^2 = 0.28$) and Mn ($r^2 = 0.27$) in the A horizons, whereas in the B horizons, there are positive correlations with C_{org} ($r^2 = 0.49$), and subordinately, Fe_{tot} ($r^2 = 0.23$), and P_2O_5 ($r^2 = 0.16$).

No significant isotopic difference exists between the P-2 soil developed on Porphyroids (metarhyolites), and the P-1 and P-7 soils evolved on *Arenarie di san Vito*, due to similar mineral assemblages and ages of the two formations. The metamorphic rock-based soils exhibit a large range of $\delta^{87}Sr$ (12.5–65.9‰) and, in general, a vertical increase, which is more linear in the less evolved P-1 and P-2 soils. The P-9 soil shows a significant increase from the A1 to the A2 horizons and a slight decrease in the Btg horizons. In contrast, the carbonate-based P-6 soil shows the narrowest range of $\delta^{87}Sr$ (1.7–18.1‰) and a swinging vertical pattern; its $\delta^{87}Sr$ are higher than the value of the bedrock, and are correlated negatively with the Ca concentrations ($r^2 = 0.73$; Fig. 6). The ε_{Nd} encompass a relatively narrow range from −14.5 to −7.8, in particular in the less evolved P-1 and P-2 soils. The P-9 soil exhibits the lowermost ε_{Nd} of all the soils. The ε_{Nd} do not distinguish the carbonate-based P-6 soil from the others of the same catchment. Both the $\delta^{87}Sr$ and ε_{Nd} of the organic horizon of the P-7 soil are remarkable, as they are lower than the values of the other horizons of this soil.

Lastly, the $\delta^{87}Sr$ values of the marine aerosols average 0.02‰, and are similar to the average value of Tyrrhenian seawater ($\delta^{87}Sr = 0$‰).

5. Discussion

5.1. The sources of Sr, Nd, and Ca and the distribution of these elements in the studied soils

As bedrock minerals are by far quantitatively the most important source for the amount of Sr, Nd, and Ca released by weathering to the soil solution, and there are no data of mineral composition of dust, the distribution of these elements in the soils is thus focused on bedrock mineralogy.

Among the main Sr-bearing minerals in the bedrocks from *Arenarie di san Vito* (Scarciglia et al., 2013), Sr is particularly enriched in apatite (2875 mg/kg), whereas it is very subordinate in muscovite (88 ± 21 mg/kg), and, to lower extent, albite (19–31 mg/kg) and chlorite (17 mg/kg). As this latter mineral is not as common as the others, its Sr contribution can be negligible. Moreover, muscovite is generally extremely resistant to weathering (e.g. Lasaga, 1984; Blum and Erel, 1997) relative to apatite and plagioclase. In this context, the vertical Sr decrease observed in the soils (Fig. 2) may mean that in the upper horizons, either the Sr-bearing minerals are generally more resistant to weathering than the other phases, and/or after release from weathered minerals, Sr has been retained by sorption onto soil matrices. In contrast, the trend of vertical increase in the carbonate-based P-6 soil (Fig. 2) agrees with the dissolution of calcite in the decalcified upper horizons, being calcite the overwhelmingly abundant Sr-bearing mineral in this soil. The positive correlations of Sr versus C_{org}, Ca, and Mn in the A horizons of the metamorphic rock-based soils (Fig. 4) suggest that Sr is significantly associated with organic matter, probably via complexes, carbonates, and Mn oxi-hydroxides. The close association of Sr and C_{org} also characterizes the B horizons of these soils, although to a lower extent, suggesting persistence of the Sr link with organic matter in those layers.

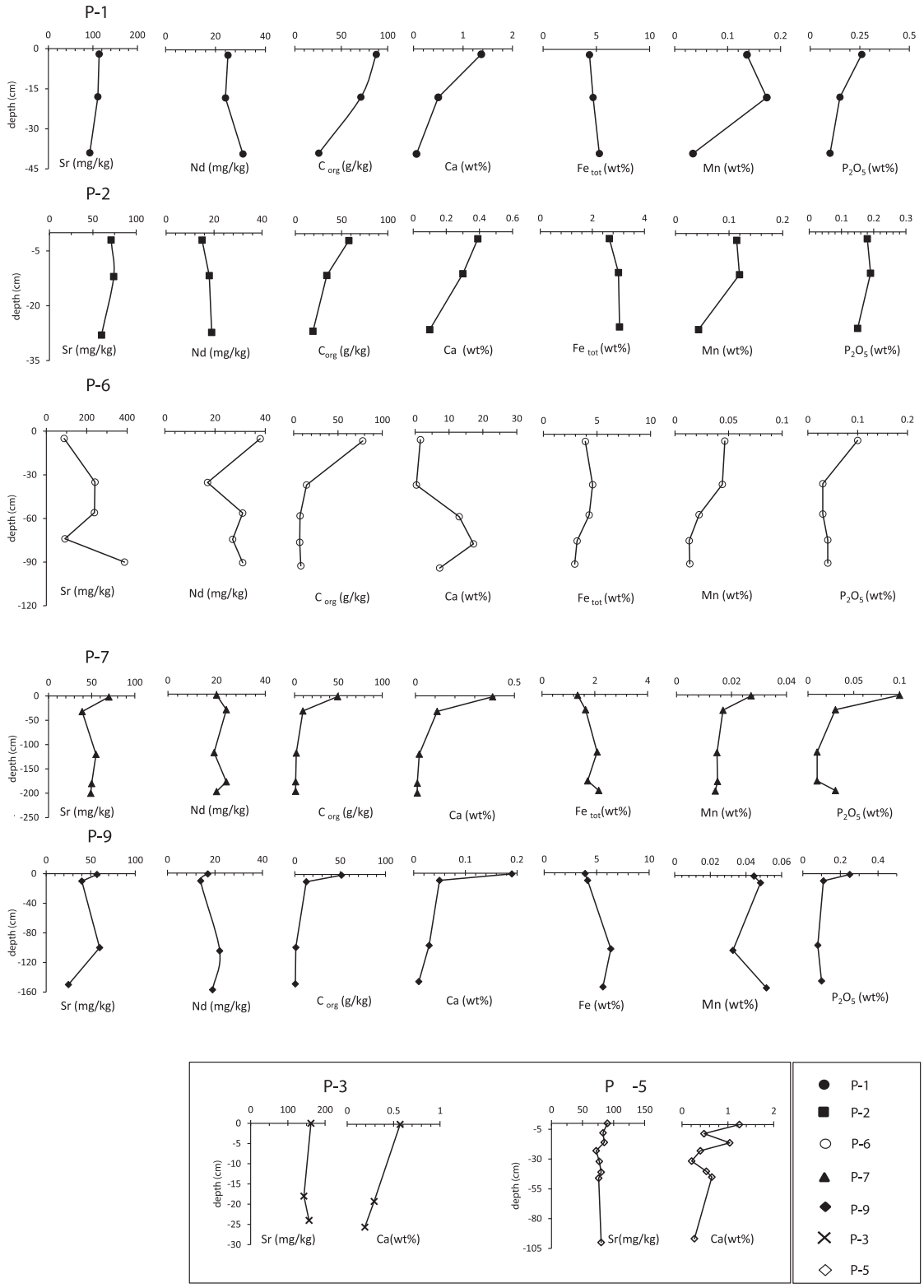

Fig. 2. The vertical variations of Sr, Nd, C_{org}, Ca, Fe_{tot}, Mn, and P_2O_5 through each soil profile from Muravera. The Sr variations with depth in the P-3 (star) and P-5 (open diamond) soils (data after Castorina and Masi, 2007, 2008) are shown for comparison.

Among the main Sm- and Nd-bearing minerals in the studied soils (Scarciglia et al., 2013), muscovite and chlorite host more Nd (5 and 3 mg/kg, respectively) than albite (<1.3 mg/kg), whereas Sm is higher in chlorite (5 mg/kg) than in both muscovite and albite (<0.7 mg/kg). However, because of the scanty abundance of chlorite, its Nd contribution to the soil solution can be neglected. No data of Nd are available for apatite, which is a major REE-bearing mineral in the soils. Nevertheless, it is known that apatite is

Table 2
The Sr and Nd isotopic ratios of the studied soils from Muravera. The Sr isotopic compositions of samples of marine aerosols, Tyrrhenian seawater, and the P-3 and P-5 soils (data after Castorina and Masi, 2007, 2008) are shown for comparison.

Soil	Horizon	$^{87}Sr/^{86}Sr \pm 2se^{*}$	$\delta^{87}Sr$ (‰)	$^{143}Nd/^{144}Nd \pm 2se^{*}$	ε_{Nd}
P-1	A1	0.721539 ± 10	17.4	0.512068 ± 8	−11.2
	A2	0.727120 ± 5	25.3	0.512111 ± 8	−10.3
	Bw	0.739807 ± 9	43.2	0.512060 ± 6	−11.3
	R	0.757643 ± 10	68.4	0.512085 ± 16	−10.8
P-2	A1	0.733327 ± 16	34.1	0.512143 ± 8	−9.7
	A2	0.737229 ± 7	39.6	0.512109 ± 9	−10.4
	Bw	0.743902 ± 7	49.0	0.512112 ± 8	−10.3
	R	0.752323 ± 16	60.9	0.512144 ± 9	−9.7
P-6	A	0.717604 ± 07	11.9	0.512090 ± 8	−11.1
	Bw1	0.722025 ± 10	18.1	0.512147 ± 11	−9.6
	Bw2	0.712084 ± 11	4.1	0.512088 ± 10	−10.8
	C1	0.710411 ± 6	1.7	0.512050 ± 8	−10.4
	Cg2	0.721380 ± 6	17.2	0.512046 ± 10	−11.6
	R	0.707780 ± 7	−2.0	0.512117 ± 9	−10.2
P-7	Oi	0.718034 ± 8	12.5	0.512036 ± 8	−11.8
	A	0.732105 ± 9	32.3	0.512153 ± 8	−9.5
	Bt1	0.749744 ± 10	57.2	0.512238 ± 9	−7.8
	Btg2	0.752475 ± 5	61.1	0.512091 ± 9	−10.7
	Btg3	0.755916 ± 4	65.9	0.512148 ± 16	−9.6
	Btg4	0.753740 ± 7	62.8	0.512169 ± 13	−9.2
P-9	A1	0.738020 ± 18	40.7	0.511944 ± 9	−13.6
	A2	0.754974 ± 7	64.6	0.511896 ± 16	−14.5
	Btg1	0.751518 ± 8	59.7	0.511947 ± 10	−13.5
	Btg2	0.752861 ± 15	61.6	0.511927 ± 12	−13.9
P-3	Oi	0.712243 ± 25	4.3		
	A	0.740619 ± 40	44.3		
	Bw	0.740629 ± 16	44.4		
	R	0.750656 ± 15	58.5		
P-5	Oi	0.725318 ± 21	22.8		
	A	0.741770 ± 11	46.0		
	2Ab	0.735684 ± 10	37.4		
	2Bwb	0.738032 ± 11	40.7		
	3Cb	0.739406 ± 24	42.6		
	4Ab1	0.738160 ± 24	40.9		
	4Ab2	0.736065 ± 25	37.9		
	5Cb	0.741263 ± 20	45.3		
Marine aerosol					
Ma-1		0.709178 ± 7	0.01		
Ma-2		0.709196 ± 14	0.04		
Ma-3		0.709174 ± 6	0.01		
Seawater					
SW-1		0.709172 ± 8	0		

* Errors refer to the two last significant digits.

generally enriched in Sm relative to Nd (e.g. Arth, 1976; Henderson, 1986; Fujimaki, 1986; Mahood and Stimac, 1990), whereas muscovite and albite display reverse patterns (e.g. Scarciglia et al., 2013; Stille et al., 2009). Another REE-bearing phosphate present in the studied soils, although of very subordinate importance (Scarciglia et al., 2011), is monazite, which generally hosts more Sm than Nd (Andrehs and Heinrich, 1998). The positive correlations of Nd and C_{org}, Ca, and Mn, respectively, in the A horizons of the soils and, to a lower extent, between Nd and C_{org} also in the B horizons suggest that Nd is significantly associated with organic matter, carbonates, and Mn oxi-hydroxides. The Nd enrichment in the A horizon of the carbonate-based P-6 soil is consistent with the decarbonatation of this horizon, which causes a passive increase of silicates and phosphates, both Nd-richer than calcite. Lastly, the very good positive correlation between Sr and Nd in the A horizons of the metamorphic rock-based soils along with the highly positive correlations of Sr and Nd versus C_{org} (Fig. 4) support association of the two elements with organic matter.

Lastly, regarding the Ca distribution, the vertical Ca decrease in the metamorphic rock-based soils (Fig. 2) is an anomalous behavior (e.g. Scarciglia et al., 2013). In fact, Ca is generally removed from the soil solution and, subordinately, precipitated downward in newly formed phases and/or adsorbed onto soil matrices. However, Ca enrichment in upper horizons has also been recorded in other uncultivated soils (e.g. Drouet et al., 2005); it might reflect a passive increase by retention by soil matrices. In particular, Ca can be taken up by plants as nutrient, and, thus, stored in organic matter, particularly more abundant in upper horizons. This hypothesis is supported by the significantly positive correlation between Ca and C_{org} in the metamorphic-based soils (Fig. 4). Moreover, the positive Ca–P_2O_5 correlation in the metamorphic rock-based soils (Fig. 4) supports that apatite is the most important phosphate in these soils. Lastly, the weakly positive correlations of Ca–Mn and Ca–Fe in the A and B horizons, respectively, suggest association of Ca with Mn and Fe oxi-hydroxides, respectively.

5.2. The sources of Sr and Nd for the Sr–Nd isotopic composition of the soils

Unlike for discussing the contents of Sr and Nd in the soils, the isotopic characteristics of all the sources of the two elements have been taken into account, as they can be significantly different, influencing deeply the isotopic composition of the soils. Among the main Sr-bearing minerals, Rb-rich muscovite releases radiogenic Sr by weathering, whereas Rb-free albite, phosphates, particularly labile monazite, and calcite release non-radiogenic Sr.

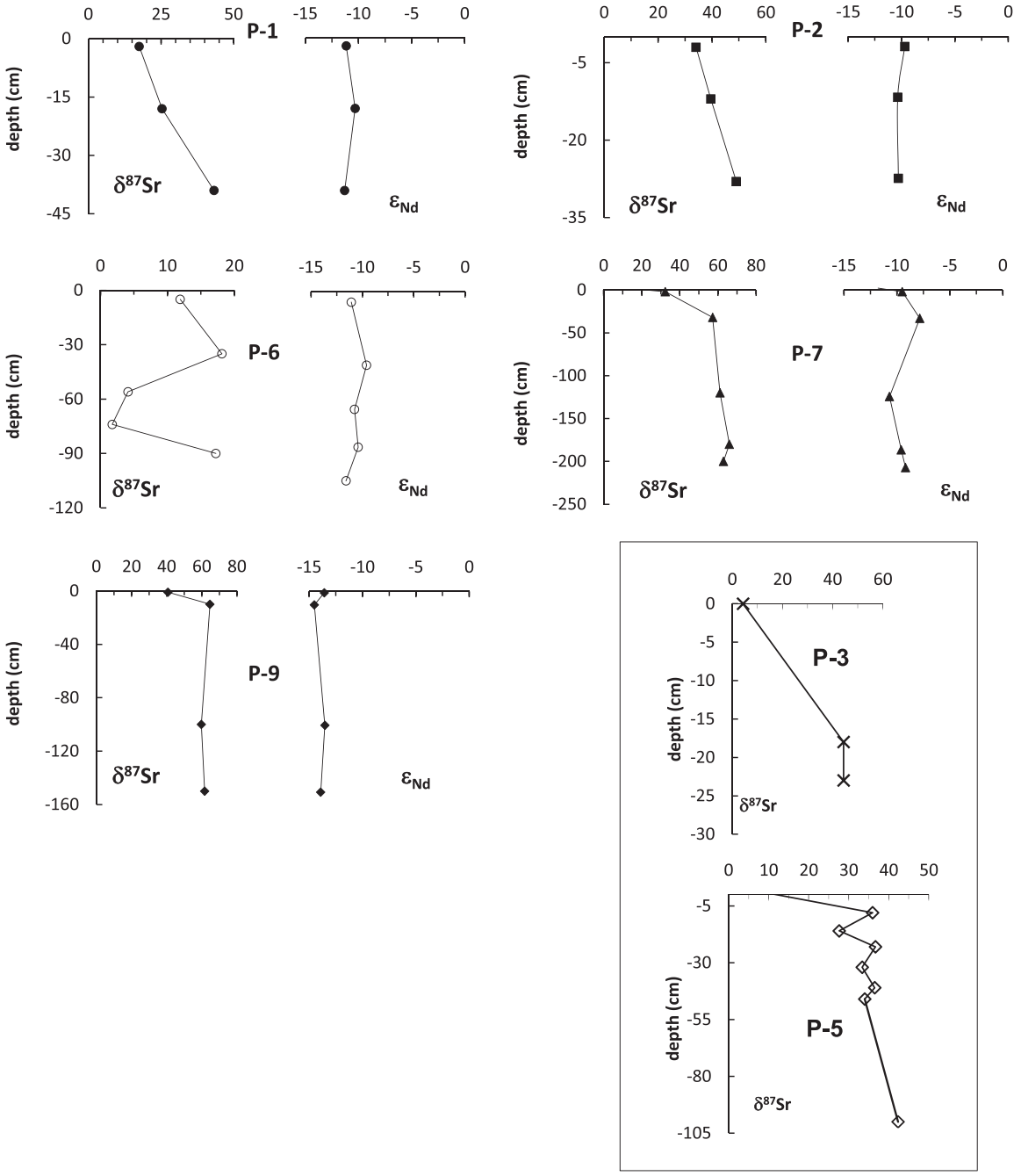

Fig. 3. The vertical variations of $\delta^{87}S$ and ε_{Nd} through each soil profile from Muravera. The variations of $\delta^{87}S$ and ε_{Nd} with depth in the P-3 and P-5 soils (data after Castorina and Masi, 2007, 2008) are shown for comparison. Symbols as in Fig. 2.

Regarding Nd, by weathering, apatite releases more radiogenic Nd than monazite, albite, muscovite, and chlorite to the soil solution. However, as monazite is labile relative to the other minerals, the weathering of this mineral may control significantly the ε_{Nd} of the soil solution. To this contribution sums up that provided by albite, which is generally less resistant to weathering than muscovite and chlorite (e.g. Swindale and Jackson, 1960; Lasaga, 1984; Blum and Erel, 1997). Sedimentary carbonates are not significant Nd contributors because of their negligible contents (e.g. Tanaka and Kawabe, 2006), and, thus, have no influence on Nd isotopic composition of soils. Lastly, there are no Sr–Nd isotopic data of illite and kaolinite, which are the mainly clay minerals in these soils (Scarciglia et al., 2011), as well as of organic matter and/or Fe–Mn oxi-hydroxides, i.e. all phases which can adsorb these elements (e.g. Dia et al., 2000). The isotopic characteristics of runoff, another potential source of Sr, but not of Nd as REE are generally very little soluble in water, are not known; however, they can be assumed to be similar to those of both the streams draining the study area (Cidu et al., 2008), i.e. the *Rio Baccu Locci* creek ($\delta^{87}Sr = 1.67–2.23‰$ or $^{87}Sr/^{86}Sr = 0.71038–071078$), and the *Rio S'Acqua Callenti* creek ($\delta^{87}Sr = 6.11–6.99‰$ or $^{87}Sr/^{86}Sr = 0.71353–0.71416$) as well as of leachates from *Arenarie di san Vito* (average $\delta^{87}Sr = 11.06‰$, Cidu et al., 2008). The marine aerosols can provide $\delta^{87}Sr$ rather similar to those of sedimentary carbonates, however, the contribution from this source as well as from runoff is very subordinate compared with that from the bedrock and dust because of much lower Sr

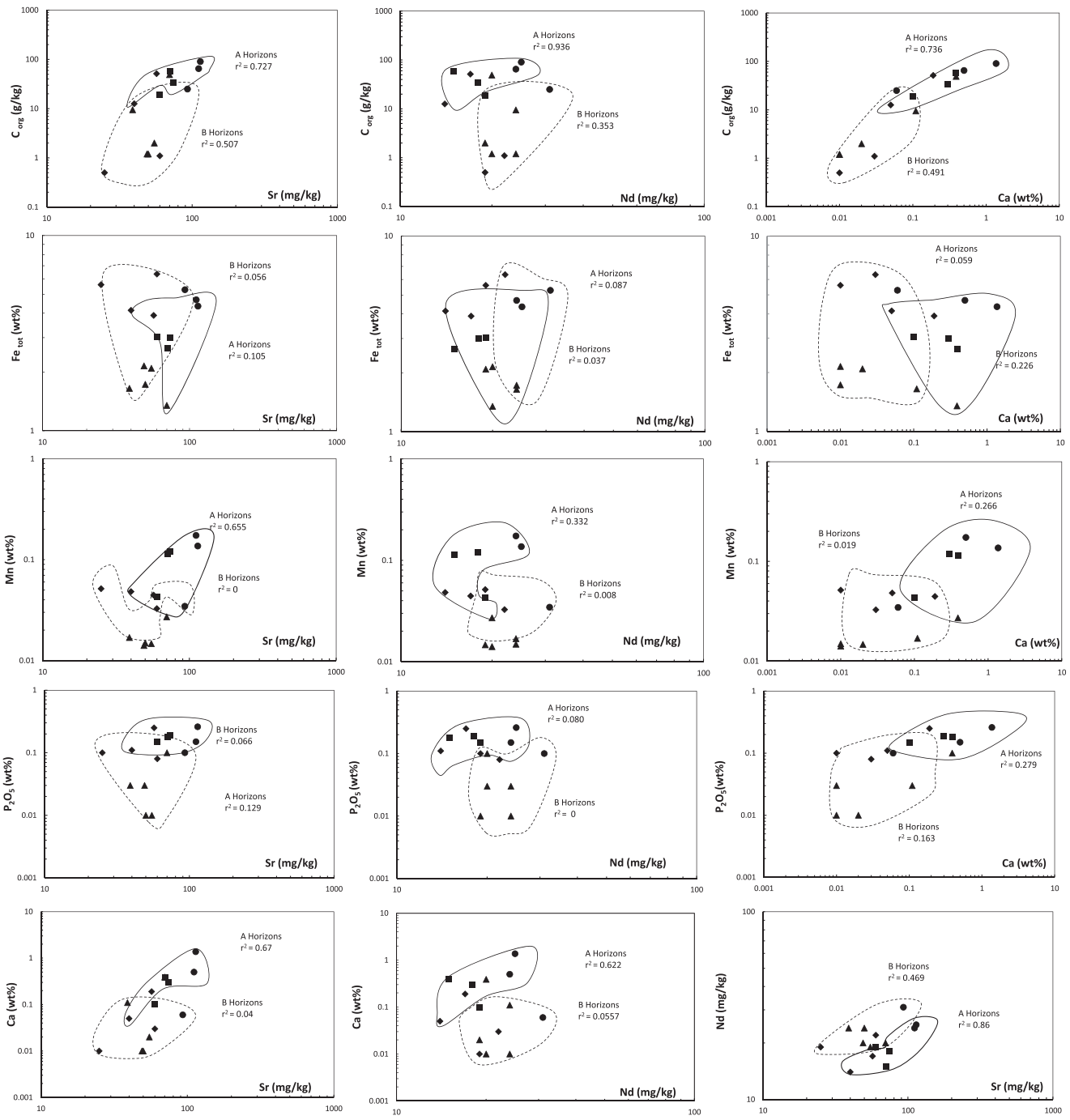

Fig. 4. The reciprocal relationships of Sr, Nd, and Ca, and between these elements and C_{org}, P_2O_5, Mn, and Fe_{tot}, respectively, in the A and B horizons of the metamorphic rock-based soils from Muravera. Symbols as in Fig. 2.

concentrations. Negligible is also the Nd contribution from marine aerosols due to the very low REE concentrations in seawater (e.g. Tanaka and Kawabe, 2006). Lastly, we deal with dust, which can be the second significant source after bedrock minerals in the study area. Dust can be supplied by either the fields contouring the studied soils, and/or the Sahara desert (e.g. Scheuvens et al., 2013 and references therein). Dust from the nearby fields is likely composed of particulate matter from *Arenarie di san Vito* and for the P-1 and P-2 soils of the *Rio Baccu Locci* catchment, from Eocene calcarenites too, although to a subordinate extent. Therefore, dust is expected to exhibit Sr isotopic composition mainly similar to *Arenarie di san Vito*, bringing in no significant variation of the $\delta^{87}Sr$ of the soils with respect to the values of bedrock minerals. In contrast, for dust from the Sahara, its contribution to the studied soils can bring in significant modification of Sr isotopic composition, as Saharan dust is characterized by lower $\delta^{87}Sr$ (6.81–25.14‰ or $^{87}Sr/^{86}Sr = 0.714–0.727$ for the central Mediterranean, Scheuvens et al., 2013, and average $\delta^{87}Sr = 18.3‰$ or $^{87}Sr/^{86}Sr$ ratio = 0.72215 for the dust deposited on Corsica, Rognon et al., 1996) than the uppermost of horizons of the studied soils, particularly those deeper and less contaminated by dust deposition. Relative to Nd isotopic composition, Saharan dust displays

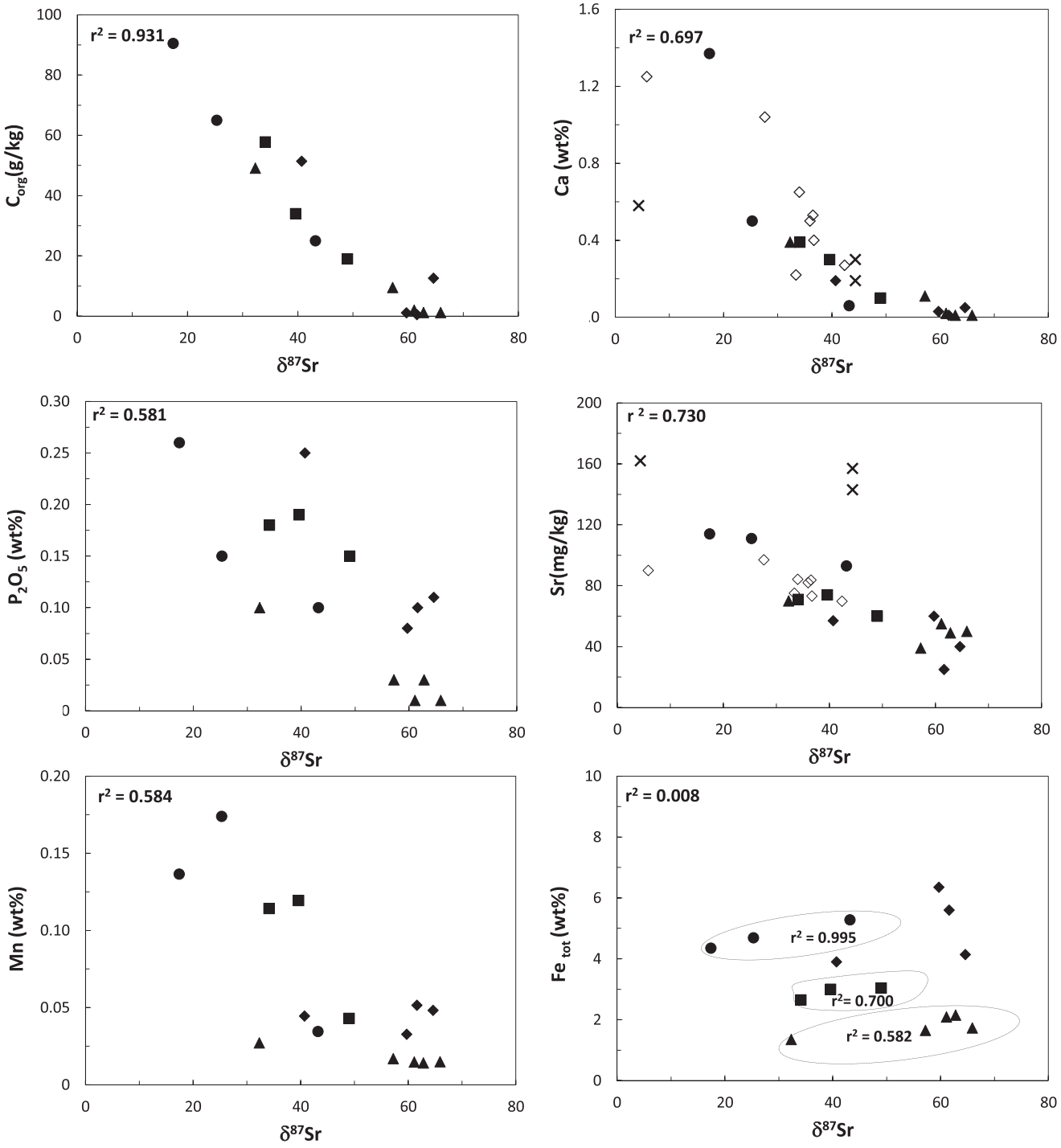

Fig. 5. The relationships between $\delta^{87}Sr$ and C_{org}, Ca, P_2O_5, Sr, Mn, and Fe_{tot}, respectively, in the metamorphic rock-based soils from Muravera. The variations of Sr, Ca, and $\delta^{87}Sr$ in the P-3 and P-5 soils (data after Castorina and Masi, 2007, 2008) are shown for comparison. Symbols as in Fig. 2.

$\varepsilon_{Nd(t)}$ from −17.1 to −8.3 (Scheuvens et al., 2013 and references therein).

5.2.1. The variations of Sr isotopic composition through the soil profiles

In the metamorphic rock-based soils, the negative correlations between $\delta^{87}Sr$ and C_{org}, Sr, Ca, Mn, and P_2O_5 (r^2 = 0.93, 0.73, 0.70, 0.58, and 0.58, respectively, Fig. 5) support that unradiogenic Sr is mainly associated with organic matter, Ca-minerals, and oxi-hydroxides of Mn. In contrast, the absence of a general correlation between $\delta^{87}Sr$ and Fe_{tot} indicates no common pattern of association of radiogenic Sr with Fe-bearing minerals/phases in the soils. However, considering the details, there are positive correlations between $\delta^{87}Sr$ and Fe_{tot} in the P-1, P-2, and P-7 soils (r^2 = 0.99, 0.70, and 0.58, respectively, Fig. 5), all from the *Rio Baccu Locci* catchment; this suggests that radiogenic Sr is mainly associated with Fe-bearing phases in these soils.

To explain the vertical increase of $\delta^{87}Sr$ in the metamorphic rock-based soils (Fig. 3), in particular, we discuss the data of the P-7 soil, which is the only soil displaying an organic horizon.

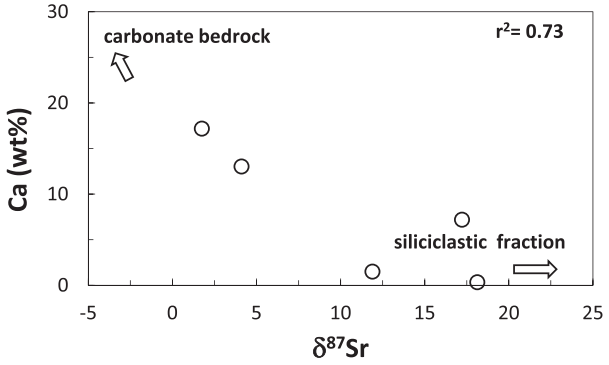

Fig. 6. The correlation between $\delta^{87}Sr$ and Ca in the carbonate-based P-6 soil samples from Muravera. The latter plot along a mixing line between the carbonate bedrock and the siliciclastic soil fraction.

Therefore, considering the $\delta^{87}Sr$ (12.5‰) of the O (organic) horizon, there is evidence that the Sr present in the soil solution and taken up by plants is relatively low radiogenic. Moreover, as the $\delta^{87}Sr$ of the O horizon is close to the average $\delta^{87}Sr$ (11.1‰, Cidu et al., 2008) of leachates from *Arenarie di san Vito*, i.e. the bedrock, this suggests that the isotopic signature of the soil solution is dominantly controlled by such a process. We now take into account the A (organic-mineral) horizon of the P-7 soil. Its $\delta^{87}Sr$ (32.3‰) results from mixing of Sr from both the organic fraction, substantially represented by the O horizon, and the inorganic fraction. The 1000/Sr versus $\delta^{87}Sr$ plot supports the hypothesis of Sr mixing from the two fractions (Fig. 7). The addition of Sr from a third end-member (carbonate), although of very subordinate importance, displaying low values of both 1000/Sr and Sr isotopic ratio may also be compatible with the observed trend. The inorganic fraction is composed of either minerals/phases inherited from the lowermost Btg4 horizon ($\delta^{87}Sr$ = 62.8‰) or atmospheric deposition. Regarding this latter source, marine aerosol ($\delta^{87}Sr$ about 0‰, Table 2) and particulate matter aerosol from carbonate rocks ($\delta^{87}Sr$ of the P-6 soil bedrock = −2.0‰, Table 2) can contribute unradiogenic Sr, but the importance of the former contributor is very subordinate. Lastly, the contribution of low radiogenic Sr from runoff ($\delta^{87}Sr$ = 1.67–6.99‰, Cidu et al., 2008) as well as that of Saharan dust of lower $\delta^{87}Sr$ (6.81–25.14‰, Scheuvens et al., 2013) than the corresponding isotopic values of any horizon apart from the O horizon can be significant. As a whole, the vertical increase of

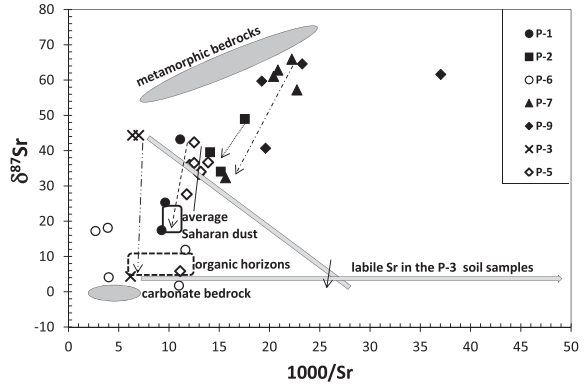

Fig. 7. The 1000/Sr ratio versus $\delta^{87}Sr$ plot for the studied soils from Muravera. The data of the P-3 and P-5 soils (Castorina and Masi, 2007, 2008) are shown for comparison. The dashed arrows show the trend of $\delta^{87}Sr$ decrease from the lower to the upper horizons in each soil profile. The solid arrows indicate the acid-leaching effect on the P-3 soil sample, yielding leachates of higher 1/Sr ratio and $\delta^{87}Sr$ similar to that of the organic horizon, but significantly lower than the values of the deeper horizons.

the $\delta^{87}Sr$ in the P-7 and other metamorphic rock-based soils may be explained by the vertical decrease of the contributions from the organic fraction, runoff, and the atmospheric input relative to the bedrock contribution.

Trying to quantify broadly the contributions of Sr from the different sources, we have carried out mass balance calculations after Stewart et al. (1998, see Appendix) for the A horizon of the P-7 soil. The relatively high proportion (about 35%) of calculated Saharan dust relative to the Sr total in the inorganic fraction of the A horizon is consistent with the findings by Erel and Torrent (2010) about such contribution to southern Spanish soils. The atmospheric input of Sr from Eocene calcarenites as well as the contribution from runoff may make the proportion of Saharan dust slightly lower.

The vertical distribution of the $\delta^{87}Sr$ in the carbonate-based P-6 soil (Fig. 3) is different from the corresponding patterns of the metamorphic rock-based soils, apart from the $\delta^{87}Sr$ increase from the A to the Bw1 horizon, as observed in the other soils. However, the isotopic values of these two horizons, which are almost totally decalcified, are higher than the value of the carbonate bedrock ($\delta^{87}Sr$ = −2.0‰, Table 2), indicating that another source of Sr of relatively high $\delta^{87}Sr$ exists beside carbonate. This source is represented by the siliciclastic fraction of this soil, particularly K-minerals. Moreover, as the isotopic values of the two horizons overlap the range of Saharan dust, a contribution from this latter source cannot be dismissed. In the lower Bw2 and C1 horizons, there is a significant decrease of $\delta^{87}Sr$ to values approaching that of the bedrock carbonate, thus evidencing the dominant contribution of Sr from low radiogenic Sr minerals, mainly calcite and, subordinately, phosphates and albite, in agreement with the high Ca contents of these horizons. Lastly, there is a significant increase of $\delta^{87}Sr$ in the lowermost Cg2 horizon, which shares similar isotopic composition with the Bw1 horizon, suggesting that the main Sr source is represented by the siliciclastic fraction. However, there is a difference between the composition of the Bw1 and Cg2 horizons, as the latter contains much more Ca than the former, in good correlation with its higher pH (Scarciglia et al., 2011) favorable to the preservation and/or deposition of carbonate. Therefore, the $\delta^{87}Sr$ of the Cg2 horizon would also result from the contribution of the carbonate fraction beyond that dominant of the siliciclastic fraction. As a whole, mixing of the Sr provided by these sources explains the negative correlation between $\delta^{87}Sr$ and Ca of this soil (Fig. 6).

5.2.2. The variations of Nd isotopic composition through the soil profiles

The relatively narrow ranges of ε_{Nd} exhibited by all the soils indicate a small fractionation of Sm and Nd. This means that either the REE-bearing minerals are scantly weathered through the profile, and/or, once REE have been released from weathered minerals, they are coherently adsorbed onto soil matrices and/or precipitated with newly-formed phases. Except for the negative ε_{Nd}–Fe_{tot} correlation in the metamorphic rock-based soils (r^2 = 0.56, Fig. 8) suggestive of association of unradiogenic Nd mainly with Fe-minerals/phases, the lack of significant correlations between ε_{Nd} and the other parameters in these soils (Fig. 8) indicates the absence of any common pattern of association of Nd with minerals/phases of defined ε_{Nd}. However, considering the details, the positive correlations between ε_{Nd} and Nd in the more evolved P-7 and P-9 soils (r^2 = 0.44 and 0.63, respectively) in contrast with the negative correlations in the less evolved P-1 and P-2 soils (r^2 = 0.46 and 0.86, respectively) indicate that, at early pedogenesis, the component of lower ε_{Nd} is associated with higher Nd concentration. This suggests the dominant contribution from monazite and albite in the less developed soils. In contrast, in the more evolved soils, radiogenic Nd is mainly associated with Nd-rich minerals/phases. This likely reflects the

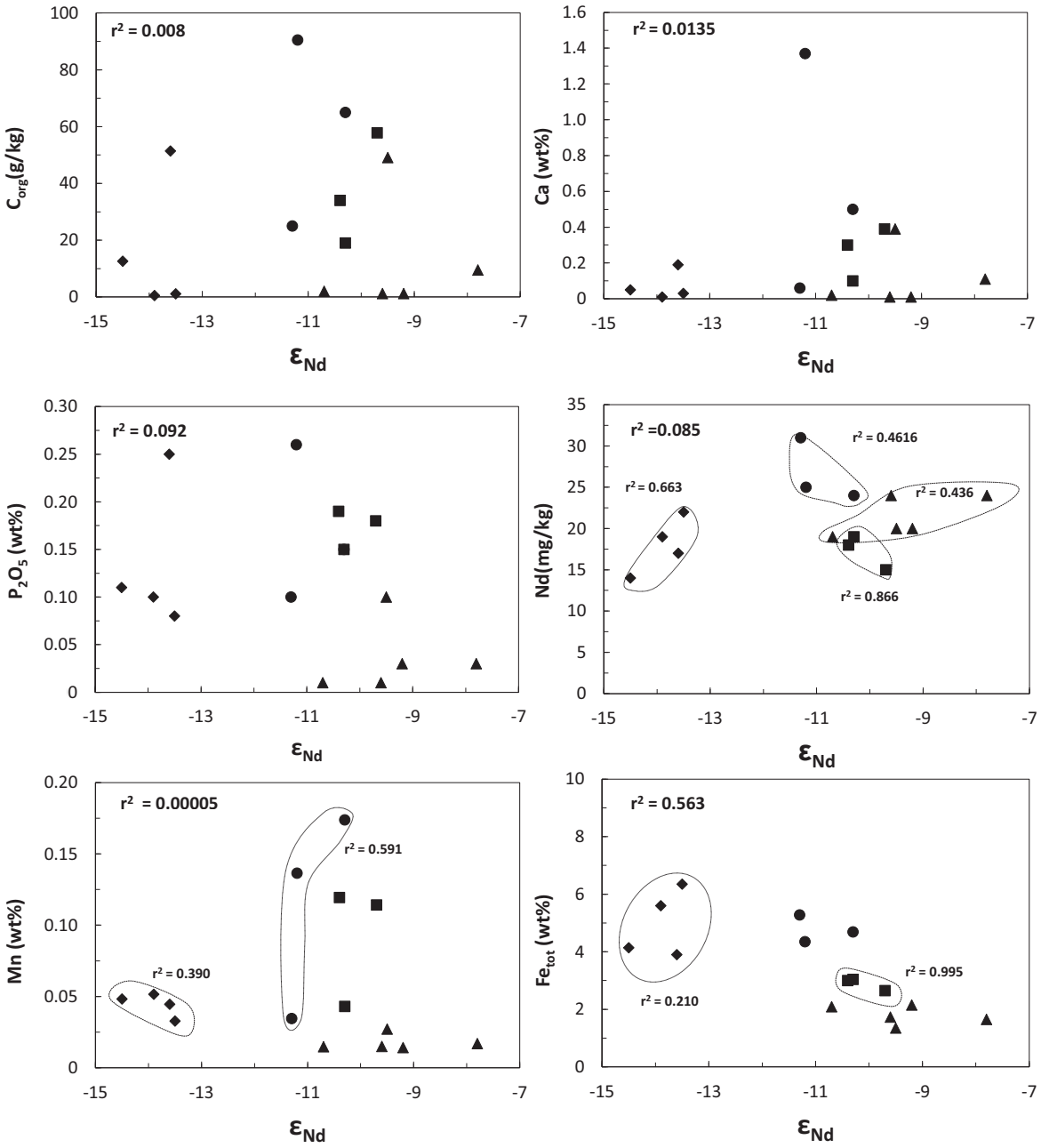

Fig. 8. The relationships between ε_{Nd} and C_{org}, Ca, P_2O_5, Nd, Mn, and Fe_{tot}, respectively, in the metamorphic rock-based soils from Muravera. Symbols as in Fig. 2.

residual character of these latter. Moreover, from Fig. 8, it appears that, unlike the negative correlation in the more evolved P-9 soil ($r^2 = 0.39$), the positive correlations between ε_{Nd} and Mn in the less developed P-1 and P-2 soils ($r^2 = 0.59$ and 0.1, respectively) suggest that, at early pedogenesis, radiogenic Nd is mainly associated with Mn oxi-hydroxides. In contrast, the positive correlation between ε_{Nd} and Fe_{tot} for the more evolved P-9 soil ($r^2 = 0.21$) as well as the negative correlation of the less evolved P-2 soil ($r^2 = 0.95$) shown in Fig. 8 indicate association of radiogenic Nd with Fe oxi-hydroxides at advanced pedogenesis.

The vertical variations of ε_{Nd} in the soils (Fig. 3) suggest either the selective release of Nd from bedrock minerals by weathering, and/or an external input. Taking into account the P-7 soil, which is also the only one displaying larger ε_{Nd} variations with depth, and in particular the ε_{Nd} (−11.8) of the O horizon, it appears that the Nd present in the soil solution and taken up by plants is low radiogenic. We now consider the ε_{Nd} (−9.5) of the A horizon, which, as for Sr, results from mixing of Nd from both the organic and inorganic fractions. However, the close values of the A and the lowermost Btg4 horizons (this latter $\varepsilon_{Nd} = -9.2$) indicate that the bulk of Nd of the A horizon is provided by bedrock minerals. Nevertheless, the contribution from Saharan dust cannot be dismissed, although there is overlap of the values of both the soil bedrock and Saharan dust ($\varepsilon_{Nd(t)}$ from −17.1 to −8.3, Scheuvens et al., 2013 and references therein). The lower value of the Btg2 horizon relative to the others may suggest resistance of phosphates and albite to weathering due to partially impeded drainage.

Lastly, considering that phosphates and, subordinately, silicates are the main sources of Nd, this may explain why the carbonate-based P-6 soil, particularly its decalcified upper horizons, displays

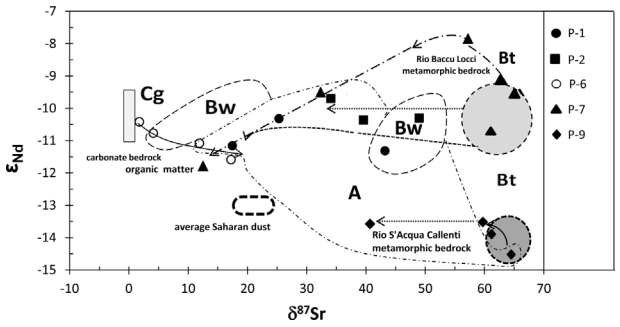

Fig. 9. The $\delta^{87}Sr$ versus ε_{Nd} plot for the samples from the different horizons of the studied soils from Muravera. The fields of reference bedrocks and average Saharan dust (Grousset et al., 1998; Grousset and Biscaye, 2005) are shown for comparison. The dashed arrows show the trend of the isotopic values from the lower to the upper horizons in each soil profile. The contour lines delimitate approximately the overall fields of the data from the A and Bw horizons.

ε_{Nd} similar to the metamorphic rock-based soils from the same catchment.

5.3. The Sr–Nd isotopic relationship in the studied soils

Fig. 9 shows the plot of $\delta^{87}Sr$ versus ε_{Nd} for all the soils. The field of the *Rio Baccu Locci* metamorphic bedrock has been drawn after the isotopic values of the P-1 and P-2 bedrocks, whereas the field of the carbonate bedrock has been defined after the P-6 bedrock. Lastly, as the isotopic characteristics of the P-9 soil bedrock are unknown, it has been assumed that this latter displays similar $\delta^{87}Sr$ but lower ε_{Nd} than the respective values of the bedrocks of the *Rio Baccu Locci* soils. From Fig. 9, no general correlation is apparent for all the soils, in agreement with the fact that Sr and Nd do not share similar geochemical behaviors. In particular, higher mobility of Sr relative to Nd may explain the larger range of $\delta^{87}Sr$ compared with that narrower of ε_{Nd} in the soils. Moreover, it appears that all the data plot between the two potential sources of Sr and Nd of the study area, i.e. rocks, and organic matter and/or average Saharan dust. Considering the details, the carbonate-based P-6 soil samples display no correlation between the isotopes of Sr and Nd if all the horizons are taken together, but, if sample Bw1 is disregarded, the others exhibit a highly negative correlation ($r^2 = 0.96$). This confirms that, in general, the isotopic composition of the different horizons of this soil results from mixing of the two elements in different proportions from both the carbonate and silicate fractions. In contrast, the metamorphic rock-based soils are characterized by more complex correlations, although there is a generally systematic decrease of $\delta^{87}Sr$ from the lower to the upper horizons at substantially steady ε_{Nd}, typically for the P-1, P-2, and P-9 soils. In contrast, in the Btg horizons of the metamorphic rock-based P-7 soil, there is a small increase of ε_{Nd} upward at rather steady $\delta^{87}Sr$ compared with the lower values of the upper horizons. This suggests weathering of albite and phosphates in the upper Btg horizons relative to muscovite of higher ε_{Nd}, in agreement with stronger resistance of the latter mineral.

Lastly, summarizing the variations of the $\delta^{87}Sr$ and ε_{Nd} in both the samples and horizons, from Fig. 9, it appears a rather well defined sample zonation moving from the middle of the plot, where the samples from the A horizons mainly cluster, toward the outer areas where the samples from the B and C horizons, and the metamorphic/carbonate bedrocks plot. This reflects the progressively both lower weathering rate and decrease of abundance of organic matter with depth in the soils.

5.4. Comparison with other soils from Muravera

It is interesting to compare the $\delta^{87}Sr$ of the soils studied in this paper with those of two other soils from the Muravera area (Fig. 1) (Castorina and Masi, 2007, 2008), also developed on Holocene deposits from *Arenarie di san Vito* (Scarciglia et al., 2011, 2013). The classification after US Soil Taxonomy (Scarciglia et al., 2011) along with the available physical–chemical parameters of the two soils (Castorina and Masi, 2007, 2008) are reported in Table 1. In particular, the P-3 soil, which is located on a hill slope next to the P-9 soil in the *Rio S'Acqua Callenti* catchment, is comparatively less evolved (Castorina and Masi, 2008). It exhibits a depth <50 cm, an O-A-Bw-R profile, and is covered by scarce vegetation, which has notably limited the pedogenesis. In contrast, the P-5 soil, which is composed of a buried soil topped by a neo-soil, occurs downhill the P-7 soil on a fluvial terrace of the *Rio Baccu Locci* catchment covered by the vegetation (Castorina and Masi, 2007). The vertical distributions of Sr and Ca in the P-3 soil and the P-5 neo-soil (Fig. 2) are generally similar to those of the other metamorphic rock-based soils, therefore, the behaviors of Sr and Ca appear to reflect common pedogenic patterns. In contrast, Sr and Ca display different distributions in the buried P-5 soil, suggesting the patterns have changed through time.

The P-3 soil exhibits a vertical increase of the $\delta^{87}Sr$ similar to the most of the other metamorphic rock-based soils (Fig. 3), supporting the common pedogenic process. Castorina and Masi (2008) explained this isotopic pattern as due to the decreasing Sr contribution with depth from an external reservoir. However, it cannot also be neglected the decreasing Sr contribution with depth from organic matter of low $\delta^{87}Sr$. Unlike the other metamorphic rock-based soils, the P-5 soil exhibits a swinging vertical isotopic pattern, which looks similar for the two sub-soils, suggesting the same Sr provenance through time. Lastly, it is worth noting that the O horizons of both the P-3 and P-5 soils display significantly lower $\delta^{87}Sr$ (4.3 and 5.8‰, respectively) than the corresponding horizon of the P-7 soil (12.5‰). These lower $\delta^{87}Sr$ are similar to the values of groundwater from the two respective catchments (4.9 and 6.5‰ for the *Rio Baccu Locci* and the *Rio S'Acqua Callenti*, Cidu et al., 2008), indicating labile Sr in organic matter is mainly that present in the waters from the two areas. The comparatively higher $\delta^{87}Sr$ of the O horizon of the P-7 soil is consistent with the evolved pedogenesis of this soil. The common pedogenic pattern of all the metamorphic rock-based soils finds support by plotting the $\delta^{87}Sr$ of the P-3 and P-5 soils in Fig. 7, where the isotopic trends of the two profiles fit in those of the other similar soils. In particular, the O horizons of the P-3, P-5, and P-7 soils plot close to average Saharan dust, supporting the inferred Sr contribution from such a source.

Lastly, Fig. 7 shows sketchy (solid arrows) the acid-leaching effect on the P-3 soil (Castorina and Masi, 2008). Whether acid leaching may simulate to some extent the pedogenic processes taking place in this soil, the information is interesting. In fact, the arrows show that the leachates from the different horizons of this soil display higher 1000/Sr ratios and $\delta^{87}Sr$ similar to that of the organic horizon but significantly lower than the values of the deeper horizons. This indicates that labile Sr derives from the dissolution of minerals of low radiogenic Sr.

5.5. Comparison with other soils developed on similar bedrocks

There are a few isotopic data of either Sr and Nd available for soils developed on metasedimentary rocks and, in general, acidic rocks similar to the protoliths of the bedrocks here studied. In such context, Martin and McCulloch (1999) measured higher $^{87}Sr/^{86}Sr$ ratios and lower ε_{Nd} in some soils relative to their parent metagraywacke, explaining these values as due to the addition of wind-blown dust. It is significant that the ε_{Nd} pattern is similar

to that of Sardinian soils. Aubert et al. (2002), Stille et al. (2006, 2009) and Lahd Geagea et al. (2008a) analyzed soils developed on granitoids of the Vosges, also finding significant atmospheric contributions of Sr and Nd to the soil solution. The Sr isotopic patterns in the Vosgian soils (and related HCl leachates) are characterized by a vertical increase, as observed in the Sardinian soils. Erel and Torrent (2010) found no systematic change of Sr isotopes and Sr contents with depth in two sandstone soils of southwestern Spain. The isotopic values plot along a mixing line between Saharan dust and the weathered parent granitoids. Despite some close characteristics, however, the Sardinian and Spanish soils display different vertical patterns of Sr isotopic composition. Lastly, Roig et al. (2006) measured the Nd isotopic ratios of organic horizons of three Brazilian soils developed on gneiss, finding no significant vertical change, as observed for the Sardinian soils, but a significant variation in Nd contents, likely because of the REE mobilization with clay minerals from the A to the B horizon.

6. Conclusions

The application of the Sr–Nd isotopic systematics has enabled us to outline the pedogenesis and geochemical evolution of the studied soils under favorable conditions of virtually no pollution. In particular, the main results of this paper can be summarized as follows:

The Sr isotopic composition of the soils appears to be mainly controlled by the selective mineral weathering. In particular, the weathering of calcite, albite, and phosphates affects significantly the $\delta^{87}Sr$ of the upper horizons of the soils, releasing low radiogenic Sr to the soil solution. This Sr can be taken up by plants, as indicated by the $\delta^{87}Sr$ of the O horizon of the P-3, P-5, and P-7 soils. Moreover, the input of Saharan dust can also contribute significantly low radiogenic Sr to the upper horizons of the soils, whereas the contributions of low radiogenic Sr from marine aerosol and runoff are subordinate. Calculations carried out in particular for the A horizon of the P-7 soil suggest that the organic fraction provides about 29 wt% of the total Sr contained in this horizon. The remainder is supplied by the inorganic fraction, of which Saharan dust would provide about 42 wt%. Lastly, the $\delta^{87}Sr$ of the carbonate-based soil reflect the variable contributions of both non-radiogenic Sr from carbonates, albite, and phosphates, and radiogenic Sr from the siliciclastic fraction of this soil, particularly K minerals.

The Nd isotopic composition confirms the small mobility of Sm and Nd, in agreement with the common behavior of REE during rock weathering. The isotopic comparison of the A horizon and the bedrock of the P-7 soil suggests that the uppermost of Nd is provided by phosphates and albite. The contribution of Saharan dust to the inorganic fraction of the A horizon of this soil cannot be evaluated because of the isotopic overlap with the soil bedrock.

Lastly, this isotopic study has in particular allowed for evaluating the potential proportion of the aeolian contribution from the Sahara to the soils of south-eastern Sardinia. This corroborates the findings of Erel and Torrent (2010), providing new data on the diffusion of Saharan dust through the central-western Mediterranean.

As a whole, the data-base of Sr and Nd isotopes here presented can be useful for monitoring the environmental evolution in southern Sardinia through time, and may inspire similar studies elsewhere. In fact, as the environment is going under significant stress in several areas, setting up a data-base, possibly not limited to Sr and Nd only, appears to be an urgent task of the concerned Public Administrations.

Acknowledgments

The authors are grateful to the reviewers and Associate Editor Dr. S. Norra for improving the quality of the paper. This work was partially supported by grants of the project Prin 2004 – Geobasi – Geochemical baselines of Italy (coordinator: G. Ottonello, University of Genova; local responsible: Francesca Castorina, University of Rome "La Sapienza").

Appendix A.

In order to calculate the Sr contribution from the inorganic fraction to the A horizon of the P-7 soil, we use the formula (1) after Stewart et al. (1998) for a mixture of two components, i.e. the organic (OF) and inorganic (IF) fractions:

$$\frac{\delta^{87}Sr_A - \delta^{87}Sr_O}{d^{87}Sr_{IF} - \delta^{87}Sr_O} \times 100 = \%IF \quad (1)$$

where $\delta^{87}Sr_{IF}$ and $\delta^{87}Sr_O$ are the isotopic ratios of the IF and OF, respectively, and $\delta^{87}Sr_A$ is the isotopic ratio of the A horizon (32.3‰). The OF can be broadly represented by the O horizon ($\delta^{87}Sr_O = 12.5‰$), whereas the IF is composed of phases hosted by both the soil bedrock (i.e. the Btg4 horizon, δ^{87} Sr = 62.8‰) and Saharan dust (average δ^{87} Sr = 18.3‰ for that deposited on Corsica after Rognon et al., 1996).

Therefore, assuming equal Sr contributions from the three sources, it results:

$$\frac{32.3 - 12.5}{(62.8 + 18.3)/2 - 12.5} \times 100 = 70.6\% \quad IF \quad (\text{or } OF = 29.4\%)$$

Within the IF, the proportion of Saharan dust would represent about 35.3% of the Sr total.

However, if it is assumed that the Sr concentrations contributed by both the Btg4 horizon and Saharan dust are probably significantly different (for instance 48 and 121 mg/kg, respectively, the latter figure after Rognon et al., 1996), the proportion of the Saharan component would be about 42.3% of the Sr total of the IF.

References

Åberg, G., Jacks, G., Hamilton, P.J., 1989. Weathering rates and $^{87}Sr/^{86}Sr$ ratios: an isotopic approach. J. Hydrol. 109, 65–78.
Andrehs, G., Heinrich, W., 1998. Experimental determination of REE distributions between monazite and xenotime: potential for temperature-calibrated geochronology. Chem. Geol. 149, 83–96.
Andreucci, S., Bateman, M.D., Zucca, C., Kapur, S., Akşit, İ., Dunajko, A., Pascucci, V., 2012. Evidence of Saharan dust in upper Pleistocene reworked palaeosols of north-west Sardinia, Italy: palaeoenvironmental implications. Sedimentology 59, 917–938.
Arimoto, R., Duce, R.A., Savoie, D.L., Prospero, J.M., 1992. Trace elements in the aerosol particles from Bermuda and Barbados: concentrations, sources, and relationships to aerosol sulphate. J. Atmos. Chem. 14, 457.
Arth, J.G., 1976. Behavior of trace elements during magmatic processes—a summary of theoretical models and their applications. J. Res. U.S. Geol. Surv. 4, 41–47.
Aubert, D., Stille, P., Probst, A., Gauthier-Lafaye, F., Pourcelot, L., Del Nero, M., 2002. Characterization and migration of atmospheric REE in soils and surface waters. Geochim. Cosmochim. Acta 66, 3339–3350.
Blum, J.D., Erel, Y., 1997. Rb–Sr isotope systematics of a granitic soil chronosequence: the importance of biotite weathering. Geochim. Cosmochim. Acta 61, 3193–3204.
Borg, L.E., Banner, J.L., 1996. Neodymium and strontium isotopic constraints on soil sources in Barbados, West Indies. Geochim. Cosmochim. Acta 60, 4193–4206.
Bullen, T., White, A., Blum, A., Harden, J., Schulz, M., 1997. Chemical weathering of a soil chronosequence on granitoid alluvium: II. Mineralogic and isotopic constraints on the behavior of strontium. Geochim. Cosmochim. Acta 61, 291–306.
Capo, R.C., Stewart, B.W., Chadwick, O.A., 1998. Strontium isotopes as tracers of ecosystem processes: theory and methods. Geoderma 82, 197–225.
Carmignani, L., Conti, P., Barca, S., Cerbai, N., Eltrudis, A., Funedda, A., Oggiano, G., Patta, E., 2001. Note Illustrative della Carta Geologica d'Italia alla scala 1:50. 000 "Foglio 549-Muravera. Servizio Geologico d'Italia, Roma, pp. 1–140.
Castorina, F., Masi, U., 2007. Use of Sr isotopes to constrain Sr (and Ca) sources in a Mediterranean soil profile near Muravera (SE Sardinia). Acta Vulcanol. 19, 107–112.
Castorina, F., Masi, U., 2008. The Sr-isotope composition of soils: a case study from Muravera (SE Sardinia, Italy). J. Geochem. Expl. 96, 86–93.
Cidu, R., Caboi, R., Biddau, R., Petrini, R., Slejko, F., Flora, O., Stenni, B., Aiuppa, A., Parello, F., Valenza, M., 2008. Caratterizzazione idrogeochimica ed isotopica e valutazione della qualità delle acque superficiali e sotterranee campionate nel Foglio 549 Muravera. In: Ottonello, G. (Ed.), Geobasi. Pacini Pisa, pp. 149–183.

DePaolo, D.J., Wasserburg, G.J., 1976. Nd isotopic variations and petrogenetic models. Geophys. Res. Lett. 3, 249–252.
Dia, A., Gruau, G., Olivié-Lauquet, G., Riou, C., Molénat, J., Curmi, P., 2000. The distribution of rare-earth elements in groundwaters: assessing the role of source-rock composition, redox changes and colloidal particles. Geochim. Cosmochim. Acta 64, 4131–4151.
Drouet, Th., Herbauts, J., Gruber, W., Demaiffe, D., 2005. Strontium isotope composition as a tracer of calcium sources in two forest ecosystems in Belgium. Geoderma 126, 203–223.
Erel, Y., Torrent, J., 2010. Contribution of Saharan dust to Mediterranean soils assessed by sequential extraction and Pb and Sr isotopes. Chem. Geol. 275, 19–25.
Fujimaki, H., 1986. Partition coefficients of Hf, Zr and REE between zircon, apatite and liquid. Contrib. Mineral. Petrol. 94, 42–45.
Genova, N., Meloni, S., Oddone, M., Melis, P., 2001. On the origin of some red soils from Sardinia (Italy): a neutron activation analysis investigation. J. Radioanal. Nucl. Chem. 249, 355–360.
Green, G.P., Bestland, E.A., Walker, G.S., 2004. Distinguishing sources of base cations in irrigated and natural soils: evidence from strontium isotopes. Biogeochemistry 68, 199–225.
Grousset, F.E., Parra, M., Bory, A., Martinez, P., Bertrand, P., Shimmield, G., Ellam, R.M., 1998. Saharan wind regimes traced by the Sr–Nd isotopic composition of subtropical Atlantic sediments: last glacial maximum vs. today. Quat. Sci. Rev. 17, 395–409.
Grousset, F.E., Biscaye, P.E., 2005. Tracing dust sources and transport patterns using Sr, Nd and Pb isotopes. Chem. Geol. 222, 149–167.
Henderson, P., 1986. Inorganic Geochemistry. Pergamon Press, Oxford, pp. 1–353.
Kurtz, A.C., Derry, L.A., Chadwick, O.A., 2001. Accretion of Asian dust to Hawaiian soils: isotopic, elemental, and mineral mass balances. Geochim. Cosmochim. Acta 65, 1971–1983.
Lahd Geagea, M., Stille, P., Gauthier-Lafaye, F., Millet, M., 2008a. Tracing of industrial aerosol sources in an urban environment using Pb, Sr and Nd isotopes. Environ. Sci. Technol. 42, 692–698.
Lahd Geagea, M., Stille, P., Gauthier-Lafaye, F., Perrone, Th., Aubert, D., 2008b. Baseline determination of the atmospheric Pb, Sr and Nd isotopic compositions in the Rhine valley, Vosges mountains (France) and the Central Swiss Alps. Appl. Geochem. 23, 1703–1714.
Lasaga, A.C., 1984. Chemical kinetics of water-rock interactions. J. Geophys. Res. 89 (B6), 4009–4025.
Lawrence, C.R., Neff, J.C., Farmer, G.L., 2011. The accretion of aeolian dust in soils of the San Juan Mountains, Colorado, USA. J. Geophys. Res. 116, F02013, http://dx.doi.org/10.1029/2010JF001899
Le-Bolloch, O., Guarzoni, S., Molinardi, E., 1996. Atmosphere ocean mass fluxes at two coastal sites in Sardinia 39–41 degrees N, 8–10 degrees E. In: Guarzoni, S., Chester, R. (Eds.), The Impact of Desert Dust Across the Mediterranean. Kluwer Academic Publishing, Dordrecht, pp. 217–222.
Mahood, G.A., Stimac, J.A., 1990. Trace-element partitioning in pantellerites and trachytes. Geochim. Cosmochim. Acta 54, 2257–2276.
Martin, C.E., McCulloch, M.T., 1999. Nd-Sr isotopic and trace element geochemistry of river sediments and soils in a fertilized catchment, New South Wales, Australia. Geochim. Cosmochim. Acta 63, 287–305.
Moulin, C., Lambert, C.E., Dulac, F., Dayan, U., 1997. Control of atmospheric export of dust from North Africa by the North Atlantic oscillation. Nature 387 (June), 691–694.
Nakano, T., Yokoo, Y., Nishikawa, M., Koyanagi, H., 2004. Regional Sr–Nd isotopic ratios of soil minerals in northern China as Asian dust fingerprints. Atmos. Environ. 38, 3061–3067.
Nicolás, J., Chiari, M., Crespo, J., Orellana, I.G., Lucarelli, F., Nava, S., Pastor, C., Yubero, E., 2008. Quantification of Saharan and local dust impact in an arid Mediterranean area by the positive matrix factorization (PMF) technique. Atmos. Environ. 42, 8872–8882.
Öhlander, B., Ingri, J., Land, M., Schöberg, H., 2000. Change of Sm/Nd isotope composition during weathering of till. Geochim. Cosmochim. Acta 64, 813–820.
Pett-Ridge, J.C., Derry, L.A., Kurtz, A.C., 2009. Sr isotopes as a tracer of weathering processes and dust inputs in a tropical granitoid watershed, Luquillo Mountains, Puerto Rico. Geochim. Cosmochim. Acta 73, 25–43.
Poszwa, A., Ferry, B., Dambrine, E., Pollier, B., Wickman, T., Loubet, M., Bishop, K., 2004. Variations of bioavailable Sr concentration and $^{87}Sr/^{86}Sr$ ratio in boreal forest ecosystems. Role of biocycling, mineral weathering and depth of root uptake. Biogeochemistry 67, 1–20.
Ricther, F.M., DePaolo, D.J., 1987. Numerical models of diagenesis and the Neogene Sr isotopic evolution of seawater from DSDP 590B. Earth Planet. Sci. Lett. 83, 27–38.
Rognon, P., Coudé-Gaussen, G., Revel, M., Grousset, F.E., Pedemay, P., 1996. Holocene Saharan dust deposition on the Cape Verde Islands: sedimentological and Nd–Sr isotopic evidence. Sedimentology 43, 359–366.
Roig, H.L., Dantas, E.L., Meneses, P.R., 2006. The effects of weathering process on Sm-Nd isotopic signatures in soil and sediments in the Queluz watershed, Paraíba do Sul river system, SE Brazil. In: Short Papers—IV South American Symposium on Isotope Geology, 24–27 April, 2006, Punta del Este—Uruguay, pp. 476–479.
Scarciglia, F., Tuccimei, P., Vacca, A., Barca, D., Pulice, I., Salzano, R., Soligo, M., 2011. Soil genesis, morphodynamic processes and chronological implications in two soil transects of SE Sardinia: traditional pedological study coupled with laser ablation ICPP-MS and radionuclide analyses. Geoderma 162, 39–64.
Scarciglia, F., Sacchi, E., Angelone, M., Apollaro, C., Armiento, G., Barca, D., Caci, E., Carucci, V., Caruso, A.M., Castorina, F., Cremisini, C., Crovato, C., Delitala, M.C., De Rosa, R., Fornelli Genot, S., Garzetti, F., Marrone, V.A., Masi, U., Nannoni, F., Pizzetti, E., Primavera, P., Protano, G., Riccobono, F., Rossi, S., Salzano, R., Soligo, M., Taddeucci, A., Tuccimei, P., Vacca, A., Vannucci, R., Vecchio, G., Voltaggio, M., 2013. Caratteri geochimici, isotopici e mineralogici dei suoli di Muravera. In: Ottonello, G. (Ed.), Geobasi: il Foglio IGMI No. 549. Pacini Pisa, Muravera, pp. 59–85.
Scheuvens, D., Schütz, L., Kandler, K., Ebert, M., Weinbruch, S., 2013. Bulk compilation of northern African dust and its source sediments—a compilation. Earth Sci. Rev. 116, 170–194.
Sevink, J., Kummel, E.A., 1984. Eolian dust deposition on the Giara di Gesturi basalt plateau, Sardinia. Earth Surf. Processes Landforms 9, 357–364, http://dx.doi.org/10.1002/esp.3290090408
Spencer, Kh.J., De Carlo, E.H., McMurtry, G.M., 1995. Isotopic clues to sources of natural and anthropogenic lead in sediments and soils from O'ahu, Hawai'i. Pac. Sci. 49, 495–510.
Springer, U., Klee, J., 1954. Prüfung der Leistungsfähigkeit von einigen wichtigen Verfahren zur Bestimmung des Kohlenstoffs mittels Chromschwefelsaure sowie Vorschlag einer neuen Schnellmethode. J. Plant Nutr. Soil Sci. 64, 1–26.
Steinmann, M., Stille, P., 1997. Rare earth element behavior and Pb, Sr, Nd isotope systematics in a heavy metal contaminated soil. Appl. Geochem. 12, 607–623.
Stewart, B.W., Capo, R.C., Chadwick, O.A., 1998. Quantitative strontium isotope models for weathering, pedogenesis and biogeochemical cycling. Geoderma 82, 173–195.
Stille, P., Steinmann, M., Pierret, M.C., Gauthier-Lafaye, F., Chabaux, F., Viville, D., Pourcelot, L., Matera, V., Aouad, G., Aubert, D., 2006. The impact of vegetation on REE fractionation in stream waters of a small forested catchment (the Strengbach case). Geochim. Cosmochim. Acta 70, 3217–3230.
Stille, P., Pierret, M.C., Steinmann, M., Chabaux, F., Boutin, R., Aubert, D., Pourcelot, L., Morvan, G., 2009. Impact of atmospheric deposition, biogeochemical cycling and water–mineral interaction on REE fractionation in acidic surface soils and soil water (the Strengbach case). Chem. Geol. 264, 173–186.
Swindale, L.D., Jackson, M.L., 1960. A mineralogical study of soil formation in four rhyolite-derived soils from New Zealand. N.Z. J. Geol. Geophys. 3, 141–183.
Tanaka, K., Kawabe, I., 2006. REE abundances in ancient seawater inferred from marine limestone and experimental REE partition coefficients between calcite and aqueous solution. Geochem. J. 40, 425–435.
Viers, J., Wasserburg, G.J., 2004. Behavior of Sm and Nd in a lateritic soil profile. Geochim. Cosmochim. Acta 68, 2043–2054.
Vitousek, P.M., Kennedy, M.J., Derry, L.A., Chadwick, O.A., 1999. Weathering versus atmospheric sources of strontium in ecosystems on young volcanic soils. Oecologia 121, 255–259.
White, W.M., Patchett, P., 1984. Hf–Nd–Sr isotopes and incompatible element abundances in island arcs: implications for magma origins and crust–mantle evolution. Earth Planet. Sci. Lett. 67, 167–185.
Yaalon, D.H., 1997. Soils in the Mediterranean region: what makes them different? Catena 28, 157–169.